J. Nonlinear Sci. Vol. 16: pp. 201–231 (2006)
DOI: 10.1007/s00332-005-0696-3

Journal of
Nonlinear
Science

Winding Numbers and Average Frequencies in Phase Oscillator Networks

M. Golubitsky,[1] K. Josić,[1] and E. Shea-Brown[2]

[1] Department of Mathematics, University of Houston, Houston TX 77204-3008, USA

[2] Courant Institute of Mathematical Sciences and Center for Neural Science, 251 Mercer St., New York University, New York, NY 10012, USA

Received March 3, 2005; revised version accepted December 12, 2005
Online publication March 16, 2006
Communicated by S. Strogatz

Summary. We study networks of coupled phase oscillators and show that network architecture can force relations between average frequencies of the oscillators. The main tool of our analysis is the coupled cell theory developed by Stewart, Golubitsky, Pivato, and Török, which provides precise relations between network architecture and the corresponding class of ODEs in $\mathbf{R}^M$ and gives conditions for the flow-invariance of certain polydiagonal subspaces for all coupled systems with a given network architecture. The theory generalizes the notion of fixed-point subspaces for subgroups of network symmetries and directly extends to networks of coupled phase oscillators.

For systems of coupled phase oscillators (but not generally for ODEs in $\mathbf{R}^M$, where $M \geq 2$), invariant polydiagonal subsets of codimension one arise naturally and strongly restrict the network dynamics. We say that two oscillators i and j *coevolve* if the polydiagonal $\theta_i = \theta_j$ is flow-invariant, and show that the average frequencies of these oscillators must be equal. Given a network architecture, it is shown that coupled cell theory provides a direct way of testing how coevolving oscillators form *collections* with closely related dynamics. We give a generalization of these results to synchronous clusters of phase oscillators using quotient networks, and discuss implications for networks of spiking cells and those connected through buffers that implement coupling dynamics.

1. Introduction

Oscillatory phenomena are ubiquitous in nature. It is frequently possible to describe the dynamics of a stable periodically oscillating system using only the phase of the oscillation [22], [16]. While the original system evolves in $\mathbf{R}^M$, where M may be large or even infinite, the phase-reduced system evolves in $\mathbf{S}^1$, which typically simplifies the analysis considerably. For oscillatory systems coupled together to form networks [29],

the reduction to phase coordinates can also be performed [20], [17]. Examples of such reductions frequently used in neuroscience are reviewed in Appendix A.

We refer to the individual units in a network as *cells*, and their interactions determine the *architecture* of the network. The architecture is in turn represented by a directed graph, reflecting which cells are identical and how they are coupled. The precise relations between this directed graph and the equations that govern the network dynamics are discussed in [28], [15] and are reviewed in Section 5.

When the dynamics of the cells is determined by their phases, the reduced system is a network of phase oscillators whose equations have the form

$$\theta' = F(\theta). \tag{1.1}$$

Here $\theta = (\theta_1, \ldots, \theta_N) \in \mathbf{T}^N$, $F = (f_1, \ldots, f_N) \in \mathbf{R}^N$, and each coordinate satisfies $0 \leq \theta_j < 1$, so that the phase space of each oscillator is the unit interval $[0, 1]$ with endpoints identified.

The goal of this paper is to show that network architecture alone, regardless of any further structure of the underlying equations, can force relations between the winding numbers and average frequencies of cells in phase oscillator networks. The strongest result is easiest to describe for all-to-all coupled networks of identical cells. In this case, the number of oscillations, or windings around the origin, for any pair of cells and any solution differs by at most one on any time interval. Therefore, the average frequencies of the cells are equal. This kind of relation between certain pairs of cells exists in a variety of networks. In the following, we describe how these restrictions arise, and how they can be identified from a given network architecture.

The paper is organized as follows: In Section 2 we define winding numbers and average frequencies, and introduce the notion of coevolving pairs of oscillators. We also show that coevolving oscillators and those that are part of an appropriately defined collection have related winding numbers and average frequencies. In Section 3 we define "spiking" phase oscillator networks, motivated by neuroscience, and show that coevolving oscillators have related "spike counts." The next task is to determine how network architecture results in coevolving pairs of oscillators. Examples of networks that illustrate the underlying ideas are given in Section 4. The abstract network formalism of [15] is reviewed and is used to derive results for general networks in Section 5, and the notion of quotient networks is used to extend these results to synchronous clusters of oscillators in Section 6. In Section 7 we show that the same criteria for coevolution hold when the cells are coupled through intermediate "buffer" cells that could be used to model the time dependence of neural synaptic variables. We also describe networks for which cells that coevolve do so regardless of the presence of buffer cells. A brief discussion, including comments on neural applications, then brings the paper to a close. The Appendix gives an outline of the derivation of phase equations.

2. Winding Numbers and Coevolution

In this section we introduce the notions of winding number and average frequency which describe the temporal behavior of solutions of (1.1). We then show that these are related for coevolving oscillators in a network.

Let $F^L\colon \mathbf{R}^N \to \mathbf{R}^N$ denote the lift of the vector field $F\colon \mathbf{T}^N \to \mathbf{R}^N$ in (1.1). Suppose that $\theta(t)$ is a solution to (1.1) with initial condition $\theta(0) = \theta_0$. The lift of $\theta(t) \in \mathbf{T}^N$ to $\mathbf{R}^N$ is the solution to $x' = F^L(x)$ satisfying $x(0) = \theta_0$ and is denoted by $\theta^L(t)$.

The winding number of cell j for a solution to (1.1) over a time interval $\tau = [t_1, t_2]$ is the number of oscillations, or "windings" around the origin, that cell j undergoes during the interval τ. The following definition makes this precise.

Definition 2.1. Let $\theta(t)$ be a solution of (1.1) on an interval $\tau = [t_1, t_2]$. The *winding number* of $\theta_j(t)$ on the interval τ is given by

$$\rho_j^\tau = \theta_j^L(t_2) - \theta_j^L(t_1). \tag{2.1}$$

In general ρ_j^τ is not an integer. However, if $\theta(t)$ is a T-periodic solution to (1.1), then the lift satisfies

$$\theta^L(t + T) = \theta^L(t) + \rho, \tag{2.2}$$

where $\rho = (\rho_1, \ldots, \rho_N) \in \mathbf{Z}^N$ is a vector of integers. The winding number satisfies $\rho_j^{[0,T]} = \rho_j$, and is therefore an integer that equals the number of full oscillations of cell j during one period of $\theta(t)$. In the remainder of the paper, the winding number of θ_j in a periodic orbit will always refer to $\rho_j^{[0,T]} = \rho_j$, where T is the minimal period for the solution as a whole.

The winding number is closely related to the frequency of oscillation. Given an interval $\tau = [t_1, t_2]$, we define the *average frequency* ν_j^τ over τ by

$$\nu_j^\tau = \frac{\rho_j^\tau}{t_2 - t_1}. \tag{2.3}$$

If the limit

$$\nu_j = \lim_{|\tau| \to \infty} \nu_j^\tau$$

exists, we say that ν_j is the *average frequency* of cell j.

In the case of a T-periodic solution, we have

$$\nu_j = \lim_{t \to \infty} \nu_j^{[0,t]} = \lim_{t \to \infty} \frac{\rho_j^{[0,t]}}{t} = \lim_{N \to \infty} \frac{\rho_j^{[0,NT]}}{NT} = \frac{\rho_j}{T},$$

so that ν_i equals the number of oscillations per unit time. Similarly, ν_i for a nonperiodic solution is the average number of oscillations per unit time, which justifies the name "average frequency."

2.1. Coevolving Oscillators

The property of the network that imposes relations between winding numbers is described in the following definition.

Definition 2.2. Two phase oscillators i and j *coevolve* if the codimension-one torus $\{\theta \in \mathbf{T}^N\colon \theta_i = \theta_j\}$ is flow-invariant.

Proposition 2.3 proves that winding numbers for a periodic solution are equal for any pair of coevolving oscillators. In fact, more is true. In Proposition 2.4 we prove that, for arbitrary solutions on any interval, winding numbers of coevolving cells differ by at most 1. It then follows that if average frequencies are defined for two coevolving cells, then these average frequencies are equal. This type of behavior is similar to frequency locking [25], but we emphasize that in the present case "frequency" refers to the average number of full oscillations per unit time.

First we motivate these results and then give a precise proof. Since the torus $\theta_i = \theta_j$ is assumed to be flow-invariant, the projections $\theta_i(t)$ and $\theta_j(t)$ of the trajectory $\theta(t)$ are either identical or cannot cross. In other words, oscillators i and j cannot "lap" or "pass" one another. Therefore, the winding numbers ρ_i and ρ_j for a periodic orbit $\theta(t)$ must be equal. Furthermore, for a general solution on an interval τ, ρ_i^τ and ρ_j^τ can differ at most by 1, since this is the greatest extent to which the phases can be separated without passing.

Proposition 2.3. *For any pair of coevolving oscillators, the winding numbers of a periodic solution to a phase oscillator system (1.1) are equal.*

Proof. By definition, oscillators i and j coevolve if $\theta_i = \theta_j$ is flow-invariant for (1.1). It follows that the codimension-one subspace $V = \{\theta \in \mathbf{R}^N \colon \theta_i = \theta_j\}$ is also flow-invariant for the lift F^L.

If $\theta^L(t) \in V$ for some time t, then $\theta_i^L(t) = \theta_j^L(t)$ for all t, and hence the winding number $\rho_i = \rho_j$. We now assume $\theta(t) \notin V$ for all t. Without loss of generality, we may assume that $\theta_i^L(t) < \theta_j^L(t)$ for all t. It follows from (2.2) that

$$\theta_i^L(kT) = \theta_i^L(0) + k\rho_i \quad \text{and} \quad \theta_j^L(kT) = \theta_j^L(0) + k\rho_j.$$

Hence, $\theta_i^L(kT) < \theta_j^L(kT)$ implies that

$$\theta_i^L(0) < \theta_j^L(0) + k(\rho_j - \rho_i)$$

for all integers k. This statement is false if $\rho_j \neq \rho_i$. Thus coevolving oscillators have the same winding number. □

Proposition 2.3 can be extended to apply to nonperiodic solutions of (1.1) as shown in the following.

Proposition 2.4. *For any solution to a phase oscillator system (1.1) on an interval τ, the winding numbers of coevolving oscillators differ at most by 1.*

Proof. By assumption, the torus $\theta_i = \theta_j$ is flow-invariant. Therefore, as above, if $\theta_i(t_1) = \theta_j(t_1)$, then $\theta_i(t) = \theta_j(t)$ for all t so that the winding numbers on the interval τ are identical. Therefore, if the lifted solution satisfies $\theta_i^L(t_1) = \theta_j^L(t_1) + p$ for some integer p, then $\theta_i(t_1) = \theta_j(t_1)$ and the winding numbers are identical.

Next, suppose that the solution satisfies $\theta_i(t_1) \neq \theta_j(t_1)$. Then, there is an integer p such that

$$\theta_i^L(t_1) + p < \theta_j^L(t_1) < \theta_i^L(t_1) + p + 1. \tag{2.4}$$

These inequalities are strict and hold when t_1 is replaced by an arbitrary time t. It therefore follows from (2.4) that

$$p < \theta_j^L(t) - \theta_i^L(t) < p + 1.$$

In terms of the winding numbers defined by (2.1) on the interval $\tau = [t_1, t_2]$, we see that

$$|\rho_j^\tau - \rho_i^\tau| = |(\theta_j^L(t_2) - \theta_i^L(t_2)) - (\theta_j^L(t_1) - \theta_i^L(t_1))| < 1.$$

Hence, the winding numbers of oscillators i and j differ by at most 1 on τ. □

The following is an immediate corollary.

Corollary 2.5. *Suppose that oscillators i and j coevolve. If the average frequency ν_i is defined, then the average frequency ν_j is defined as well, and $\nu_j = \nu_i$.*

Moreover, for coevolving oscillators i and j, $\nu_i^\tau \approx \nu_j^\tau$ for long intervals τ. In addition, for a T-periodic solution $\theta(t)$, the individual coevolving oscillators $\theta_i(t)$ and $\theta_j(t)$ must have equal winding numbers and equal periods T, but they do not necessarily have the same minimal periods. The phenomenon of *multirhythms*, in which different cells of a network have different minimal periods, will be addressed in [11] (also see [12]).

Remark 2.6. Note that a flow-invariance condition analogous to Definition 2.2 for pairs of cells evolving in $\mathbf{R}^k$, $k \geq 2$, does not necessarily give any restrictions on winding numbers, unless phase reduction is valid (see Appendix A). The reason is that the corresponding flow-invariant subspace is of codimension k greater than one, and hence does not sufficiently obstruct trajectories.

2.2. Coevolution Is Not Transitive

We now make a curious observation. Consider the three-cell network in Figure 1. The set of equations modelling such a network is

$$\begin{aligned} \theta_1' &= f(\theta_1, \theta_2), \\ \theta_2' &= f(\theta_2, \theta_1), \\ \theta_3' &= f(\theta_3, \theta_2). \end{aligned} \tag{2.5}$$

It is easy to check that the manifolds $Y_1 = \{\theta\colon\ \theta_1 = \theta_2\}$ and $Y_3 = \{\theta\colon\ \theta_1 = \theta_3\}$ are flow-invariant; however, $Y_2 = \{\theta\colon\ \theta_2 = \theta_3\}$ is not, in general, flow-invariant. So the cell pairs $(1, 2)$ and $(1, 3)$ coevolve, whereas the cell pair $(2, 3)$ does not. Therefore, while the trajectories of cells 1 and 2, and those of 1 and 3 cannot cross on $\mathbf{S}^1$, the trajectories of 2 and 3 may cross.

This example implies that coevolution is not a transitive property, and therefore does not lead to an equivalence relation. However, Propositions 2.3 and 2.4 imply that relations between winding numbers exist for cells i and k, which do not coevolve with each other, but both coevolve with a third cell j. This is formalized in Corollary 2.8.

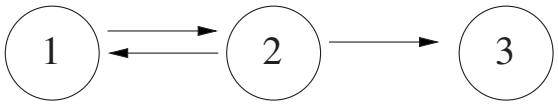

Fig. 1. A network that exhibits nontransitivity of coevolving cells.

2.3. Collections and Ordered Collections of Cells

The network of Figure 1, which demonstrates that coevolution among pairs of individual cells is not transitive, suggests two issues that we now address. First, despite this nontransitivity, we still expect some dynamical characteristics to be shared by oscillators that are related by a chain of coevolving oscillators. Second, while nontransitivity prevents us from directly using coevolution to partition a network into equivalence classes with "similar" dynamics, another relationship does permit such a partition to be specified.

Definition 2.7. Two oscillators i and j are in the same *collection* if there exists a *chain* of distinct oscillators $i = k_0, \ldots, k_{m+1} = j$ such that all pairs $(k_0, k_1), \ldots, (k_m, k_{m+1})$ coevolve; m is the length of this chain.

Note that if i and j coevolve, then the minimal length m of a chain connecting them is zero.

Collections of cells may be visualized by constructing the *collection graph* as follows. Start with N vertices, where N is the number of oscillators in the network. Construct an edge between vertices i and j if oscillators i and j coevolve. The components of the resulting graph correspond to the collections of Definition 2.7. Figure 2 gives an example of the collection graph of the network of Figure 1.

Being in the same collection is clearly a transitive relation on cells. Therefore, cells in a given network can be partitioned into a unique set of collections.

An immediate consequence of Propositions 2.3 and 2.4 is the following.

Corollary 2.8. *The collections of oscillators in a network have the following properties:*

(a) *Winding numbers of a periodic solution are equal for all cells in the same collection.*
(b) *If average frequency is defined for one cell in a collection, then it is defined for all, and this average frequency is the same for all cells in the collection.*
(c) *Let i and j be two cells in the same collection and let m be the length of the* shortest *chain of oscillators relating them. Then for a general solution, the winding numbers of cells i and j on an interval differ at most by $m + 1$.*

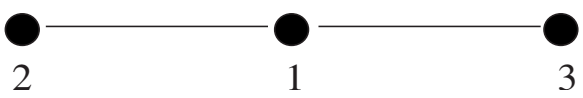

Fig. 2. The collection graph for the network of Figure 1.

Note that $m + 1$ in Corollary 2.8(c) is an upper bound. Further constraints on the dynamics exist if each pair of oscillators in a collection coevolves, as we show next.

Definition 2.9. A set of oscillators is in the same *ordered collection* if, for each pair i and j belonging to the set, i and j coevolve.

Since coevolution is generally *not* an equivalence relation, an oscillator may belong to several ordered collections at once.

The orientation of oscillators in an ordered collection is dynamically invariant, due to the flow invariance of every codimension-one torus $\{\theta\colon\ \theta_i = \theta_j\}$ for each pair of phases belonging to the ordered collection. Specifically, let $(\theta_1, \ldots, \theta_b)$ represent the phases in an ordered collection of size b . An *orientation* on this ordered collection is an ordering of the θ_j around the circle $\mathbf{T}^1$. There are $(b-1)!$ different orientations on a given ordered collection, so that there are distinct orientations only for ordered collections comprising three or more phases.

3. Phase Oscillator Models of Spiking Neuronal Networks

Phase oscillators are frequently used as models of spiking neurons, and we interpret the results of the previous section in the case of such models.

The phase equations for neuronal oscillators possess a phase φ corresponding to the point on the limit cycle (of an uncoupled neuron) where a rapid transient in voltage occurs; that is, the point at which a spike is fired [7], [4]. The phase velocity around this point must be positive for any physically plausible coupling, as neurons cannot "cross backwards" through the spike branch of their limit cycles. Thus motivated, we introduce the following:

Definition 3.1. *A* spiking cell system *is a system of coupled oscillators* $\dot{\theta}_j = f_j(\theta)$ *for* $j = 1, \ldots, N$ *where there exist* spike phases $\varphi_1, \ldots, \varphi_N$ *such that* $f_j(\theta) > 0$ *whenever* $\theta_j = \varphi_j$. *Let* $\theta(t)$ *be a solution for a spiking cell system. The cell* j spikes *at time* t *if* $\theta_j(t) = \varphi_j$.

Let $\{t_k^j\}$ be the (ordered) set of spikes for cell j. Note that requiring that $f_j(\theta) > 0$ when $\theta_j = \varphi_j$ implies that $\theta_j^L(t_{k+1}^j) = \theta_j^L(t_k^j) + 1$; in other words, θ_j must increase by a full rotation between the times it spikes. This is illustrated in Figure 3, where $\varphi_i = \varphi_j = 0$ is assumed: The horizontal lines are the lifts of $\theta_j = 0$, and the vertical lines are the lifts of $\theta_i = 0$. For a spiking system, the flow increases past these lines and winding numbers increase by one between spikes. Recalling that trajectories cannot cross $\{\theta\colon\ \theta_i = \theta_j\}$ (dashed lines), we additionally see that neuron i must fire between successive firings of neuron j, and vice versa.

Furthermore, suppose we have a periodic solution in a spiking system. The reasoning above shows that a given neuron (cell) j spikes repetitively only if the winding number ρ_j is positive, whereas neurons with rotation number 0 undergo "subthreshold" oscillations

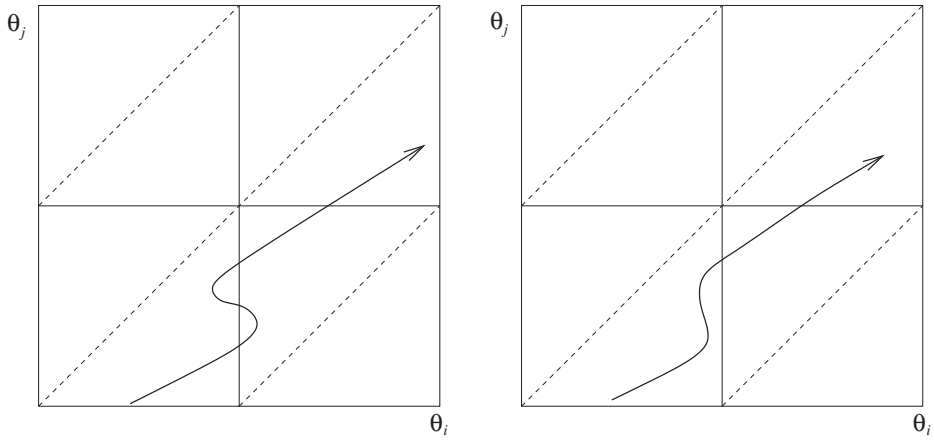

Fig. 3. Projection of representative allowed trajectories onto coordinates θ_i and θ_j for a system in which θ_i and θ_j coevolve, for a general system (left) and a spiking system (right). Dashed lines represent the lift of $\{\theta\colon\ \theta_i = \theta_j\}$ and bound the flow-invariant strips $\{\theta^L\colon\ \theta_j^L + m < \theta_i^L < \theta_j^L + m + 1\}$. The horizontal and vertical lines are the lifts of $\theta_j = 0$ and $\theta_i = 0$ respectively; when these are crossed, cell i or j spikes, respectively. For a general system, trajectories may cross a given lift of the set $\{\theta_i = 0\}$ multiple times; in spiking systems, such multiple crossings are not allowed, as $\theta_i' > 0$ on these sets. As a result, winding numbers increase by one between spikes (see text).

without spiking. Proposition 2.3 therefore implies that, for a periodic orbit, all cells that coevolve either spike or undergo subthreshold oscillations together.

We formalize the above as follows:

Proposition 3.2. *If a pair of oscillators with the same spike phase φ_0 coevolve in a spiking cell system, then either both spike coincidentally or each spikes between successive spikes of the other. Hence, their spike counts on any time interval differ by at most one, and their average spiking frequencies are equal.*

Proof. Label the two coevolving cells i and j, and let t_k^i be the time of the kth spike of θ_i as above. If $\theta_j(t_k^i) = \theta_i(t_k^i)$, then the oscillators are synchronized for all time (as in Proposition 2.4), so that all of their spikes are coincident.

Otherwise, as in Proposition 2.4, the strict inequality (2.4) holds at all times. By definition, $\theta_i^L(t_k^i) = s + \varphi_0$ for some integer s, and $\theta_i^L(t_{k+1}^i) = s + \varphi_0 + 1$. Substituting these values into (2.4) at times t_k^i and t_{k+1}^i gives

$$\theta_j^L(t_k^i) < s + \varphi_0 + p + 1 < \theta_j^L(t_{k+1}^i)\ .$$

Continuity of solution trajectories implies that θ_j^L must have crossed $s + \varphi_0 + p + 1$. Therefore, cell j spikes at some time between the successive spike times t_k^i and t_{k+1}^i of cell i. □

An immediate corollary is:

Corollary 3.3. *Consider a network of spiking oscillators with the same spike phase* φ_0.

(a) *For oscillators in the same collection, the spike counts of cells* i *and* j *over any interval differ at most by* $m+1$*, where* m *is the size of the shortest chain between them.*

(b) *No oscillator can spike twice without all others in the same ordered collection spiking in between (or coincidentally). Therefore, for a given solution, there is a fixed, possibly repeating sequence in which all such oscillators spike.*

As in Corollary 2.8(c), the number $m+1$ in Corollary 3.3(a) is an upper bound. Example 4.5 shows that this upper bound can be achieved. Corollary 3.3(b) implies that, for an ordered collection of size b, there are $(b-1)!$ distinct, dynamically invariant spiking sequences that may be displayed, depending on initial conditions.

In general, the spike phases φ_j may differ among oscillators. In Section 5 below, we introduce the notion of different oscillator *types*, and we will see that cells of the same type are the only cells that can generally be expected to coevolve. For consistency, we require that cells of the same type have the same spike phase. Therefore the assumption of Proposition 3.2 that there is a single relevant spike phase φ_0 for coevolving cells is natural, and we will tacitly take it to be true in all that follows.

Before moving to an illustrative special case, we emphasize that Propositions 2.3, 2.4, and 3.2 hold without assumptions on phase equations beyond their network architecture, and that while they were shown for phase reduced systems, they also describe the corresponding dynamics in the full state space as long as the phase reduction remains valid (see Section A.1).

3.1. Integrate and Fire Oscillators

Another type of model frequently used in neuroscience applications is the integrate and fire (IF) equation. Under certain conditions, the results of this section can also be expected to apply to networks of IF neuron models, although they are not strictly phase oscillators. The simplest form of such equation is given by the leaky integrate and fire (LIF) model:

$$\begin{aligned} v_i' &= -v_i + g(v), \\ v_i(t^+) &= \quad v_{\text{reset}}, \qquad \text{whenever } \; v_i(t) = v_\theta, \end{aligned} \tag{3.6}$$

where $g(v)$ specifies the coupling between the cells. Once the voltage v_i reaches the threshold voltage v_θ, the cell is assumed to fire (i.e., spike), and v_i is reset to v_{reset}. This implies that the points v_θ and v_{reset} can be identified when v crosses v_θ (it can be crossed only from below). On the other hand, if v_{reset} is crossed, no resetting occurs. Due to this fact, the phase space of equation (3.6) can be thought of as the branched manifold shown in Figure 3.1. The reduction of an excitable neuron model in $\mathbf{R}^N$ to an LIF equation is described in [10].

The concepts of Section 2 carry over directly to networks of IF cells. For example, consider a periodic solution in a network of such IF cells, and assume that cells i and

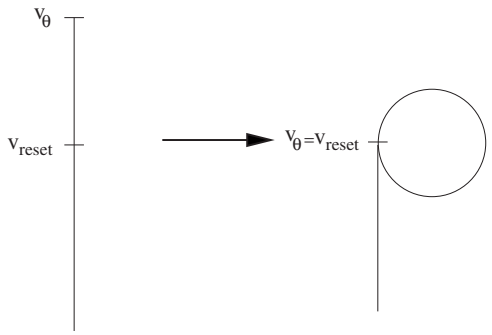

Fig. 4. The phase space of an integrate and fire (IF) oscillator is a branched manifold when the points v_θ and v_{reset} are identified. The flow on the branched manifold is defined so that any trajectory moving counterclockwise across the branch point v_{reset} continues along the straight (hyperpolarized) branch.

j coevolve. Then the branched manifold structure of the state space of the IF model implies that the only way oscillator i can have a higher winding number than oscillator j is if $v_j(t_i^k) < v_{\text{reset}}$, where t_i^k is a spike time of the ith IF neuron (that is, a time at which $v_i(t_i^k) = v_\theta$). If this is not the case, the trajectories $v_i(t)$ and $v_j(t)$ would have to cross, which is not possible. If both v_i and v_j are above v_{reset}, that is, if both v_i and v_j are on the circular part of the branched manifold in Figure 3.1 when either spikes, the arguments of the preceding section show that the winding numbers of the periodic solution must be equal for the two oscillators.

Frequently, excitatory interactions in IF networks are modelled by increasing the voltage of a postsynaptic neuron either instantaneously or through an increase in the "phase velocity" v'. In such networks, $v_i \geq v_{\text{reset}}$ for all oscillators in the network. More generally, if $v_i'(t_0) > 0$, for any t_0 such that $v_i(t_0) = v_{\text{reset}}$, all our results relating coevolution to winding numbers and spike orderings carry over directly.

If inhibitory interactions are allowed, the situation is more subtle. These are typically characterized by a synaptic "reversal potential" v_{syn} [19], which is the lowest value of a cell's voltage v at which these interactions contribute a negative term to v'. If $v_{syn} \geq v_{\text{reset}}$, then the above condition that $v_i' > 0$ when $v_i = v_{\text{reset}}$ holds, and hence so do our results relating coevolution to oscillator dynamics. However, if $v_{syn} < v_{\text{reset}}$, then this condition no longer holds (as inhibitory interactions can then force voltages below their reset values), with potentially strong consequences for the dynamics of the coupled cell network.

Therefore, care is required when defining network models using integrate-and-fire cells, and in comparing the dynamics that they produce for different parameter values. For example, in a network of two identical IF cells with identical coupling (i.e., with $\mathbf{S}_2$ symmetry), one oscillator can undergo full oscillations and spike periodically while "inhibiting" the other so that the second undergoes only subthreshold oscillation only if $v_{syn} < v_{\text{reset}}$. Proposition 2.3 states that this is not possible in a network of two identical phase oscillators or in an IF model for which the subthreshold branch is inaccessible.

Remark 3.4. Propositions 2.3 and 2.4 rely on the uniqueness of the solutions for the system (1.1). If F is discontinuous, as in the LIF model (3.6), this uniqueness may be violated. However, a simple assumption about oscillator dynamics in the neighborhood of discontinuities guarantees uniqueness of solutions, and hence that the polydiagonals $\Delta_{i,j} = \{\theta \in \mathbf{T}^N\colon \theta_i = \theta_j\}$ will be invariant for LIF models with a given architecture whenever they are invariant for smooth models with the same architecture. This assumption is as follows: let the components f_i of F be discontinuous only at the sets $\Theta_i = \{\theta\colon \theta_i = c\}$ but smooth away from these sets, and let the solutions cross these sets in the direction of increasing θ_i. A network of LIF oscillators with excitatory coupling satisfies these conditions.

4. Network Examples and Simulations

In this section we illustrate how details of network architecture not captured by symmetry can force cells to coevolve. Symmetries of the network do provide some but not all information about which cells in the network coevolve. We also illustrate by example that a network in which cells form synchronous clusters can be quotiented by identifying all cells in a cluster. As in [28], identical "node" symbols for individual cells imply identical internal dynamics, and identical arrow types imply identical coupling.

4.1. Network Symmetries and Synchrony

It is well understood that network symmetry can lead to the existence of invariant polydiagonals and synchrony. Suppose that a network has N cells $1, \ldots, N$ and that σ is a permutation of these cells. Then σ acts on $\theta \in \mathbf{T}^n$ and $F \in \mathbf{R}^N$ in (1.1) by

$$\sigma\theta = (\theta_{\sigma^{-1}(1)}, \ldots, \theta_{\sigma^{-1}(N)}) \quad \text{and} \quad \sigma F = (f_{\sigma^{-1}(1)}, \ldots, f_{\sigma^{-1}(N)}).$$

The permutation σ is a *network symmetry* if system (1.1) satisfies the *equivariance* condition

$$F(\sigma\theta) = \sigma F(\theta),$$

or, alternatively, σ is a symmetry of the network graph (see [28], [15]). For example, all-to-all coupled networks with identical couplings have full $\mathbf{S}_N$ permutation symmetry.

The *fixed-point subset* of a permutation σ is

$$\mathrm{Fix}(\sigma) = \{\theta \in \mathbf{T}^n\colon \sigma\theta = \theta\}.$$

Note that fixed-point subsets of permutations are *polydiagonals*, that is, they are defined by equality of certain cell coordinates. It is well known, and straightforward to prove, that fixed-point subsets are flow-invariant subsets [14].

4.2. All-to-all Coupled Systems

As discussed, network symmetry can imply the existence of flow-invariant subsets and hence relations between winding numbers. The simplest example occurs in all-to-all coupled systems, which have the full group of permutation symmetries $\mathbf{S}_N$.

Corollary 4.1. *In an $\mathbf{S}_N$-equivariant phase oscillator system (1.1), any pair of oscillators has winding numbers that differ by no more than one on any interval. Hence, all oscillators have the same average frequency. Furthermore, if the network is a spiking system, then between (or coincidentally with) any two subsequent spikes of a given cell, all other cells in the network must spike.*

Proof. For each pair of phases i and j, the 2-cycle $(i\ \ j)$ is in $\mathbf{S}_N$. Hence $\mathrm{Fix}(i\ \ j) = \{\theta \in \mathbf{T}^N\colon\ \theta_i = \theta_j\}$ is flow-invariant, and oscillators i and j coevolve. Therefore there is a single ordered collection containing all oscillators. □

Note that Corollary 4.1 implies that in an all-to-all coupled spiking system of identical cells, either all neurons spike or they all undergo subthreshold oscillations, *and no mixed states are possible*.

Example 4.2. Consider a six-cell all-to-all coupled phase oscillator network with equations of the form

$$\dot{\theta}_i = \omega + z(\theta_i) \sum_j \alpha_{ij} g(\theta_j), \tag{4.1}$$

where

$$z(\theta_i) = \frac{1}{2}(1 - \cos(2\pi\theta_i)),$$

which is the phase response curve for the "theta neuron" model valid near saddle-node bifurcations on an invariant curve (with $\varphi_0 = 0$) [7] ; see Section A.2. Note that all $\alpha_{ij} = \alpha$ in an all-to-all coupled network. Additionally, we choose the coupling function g to be a smoothed "pulse" with finite width:

$$g(\theta_j) = \begin{cases} 1, & \text{if } \theta_j \in [0, c], \\ e \cdot \exp\left(\dfrac{1}{((\theta_j - c)/\delta)^2 - 1}\right), & \text{if } \theta_j \in [c, c+\delta), \\ e \cdot \exp\left(\dfrac{1}{((\theta_j - 1)/\delta)^2 - 1}\right), & \text{if } \theta_j \in (1-\delta, 1], \\ 0, & \text{otherwise.} \end{cases} \tag{4.2}$$

All oscillators, while not necessarily synchronous, coevolve. Hence, as shown in Corollary 4.1, their winding numbers and spike counts over any interval differ at most by 1; furthermore, there is a single ordered collection, so all spike times are interleaved. An example is given in Figure 5.

4.3. Coevolution as a Consequence of Network Architecture

In the next example, network architecture, and not symmetry alone, results in the coevolution of cells in the network.

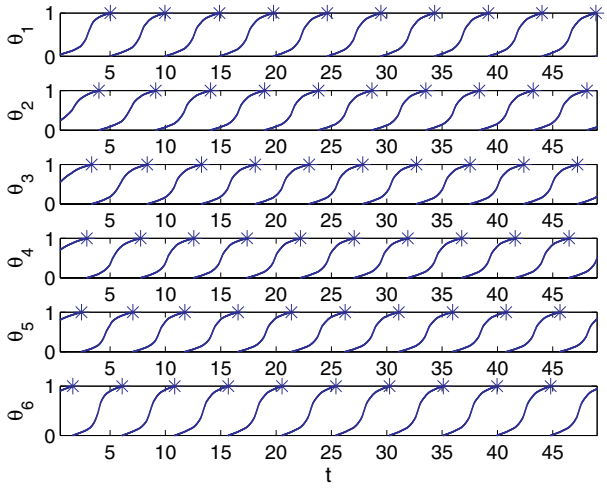

Fig. 5. Time series of a trajectory in a six cell, all-to-all coupled phase oscillator network of the form (4.1) with $c = \frac{1.42}{2\pi}$, $\delta = \frac{0.05}{2\pi}$, $\omega = \frac{0.5}{2\pi}$, and $\alpha_{ij} = \alpha = \frac{1.3}{2\pi}$. Similar results hold for a range of parameter values. Asterisks indicate spike times. Each cell spikes 10 times on the interval shown; furthermore, all spike times are interleaved, and there is a fixed, repeating sequence in which the spikes occur (see Cor. 3.3).

Example 4.3. An asymmetric three-cell network from [28] is depicted in Figure 6. The general system of differential equations associated with this network has the form

$$\begin{aligned} \theta_1' &= g(\theta_1, \theta_2, \theta_3), \\ \theta_2' &= g(\theta_2, \theta_1, \theta_3), \\ \theta_3' &= h(\theta_3, \theta_1). \end{aligned} \tag{4.3}$$

The two distinct cell types in the network result in two distinct functions g: $\mathbf{T}^3 \to \mathbf{R}$ and h: $\mathbf{T}^2 \to \mathbf{R}$. Moreover, g does not satisfy any invariance condition because cells 1 and 2 each receive two different kinds of inputs.

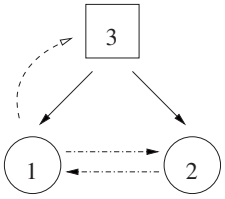

Fig. 6. A nonsymmetric three-cell network.

The torus $Y = \{\theta \in \mathbf{T}^3\colon\ \theta_1 = \theta_2\}$ is flow-invariant for all equations of the form (4.3) because the equations for θ_1' and θ_2' restricted to Y have the form

$$\theta_1' = g(\theta_1, \theta_1, \theta_3),$$
$$\theta_2' = g(\theta_1, \theta_1, \theta_3).$$

Therefore, cells 1 and 2 in this network coevolve and hence must have equal average frequencies, and winding numbers and spike counts differing by no more than one on any interval. Note that the network architecture imposes no such relations between the dynamics of oscillators 1 and 3 or 2 and 3.

As illustrated by Example 4.3, network architecture, and not merely network symmetries, can force the existence of synchronous subsets of cells. This idea is developed further in Sections 5 and 6.

The following example shows that network architecture may also force synchronous clusters within the network to have equal average frequencies. The generalization of this observation will require the machinery of quotient networks developed in [15] and reviewed in Section 6, but its essence is illustrated in the following example.

Example 4.4. Consider the six-cell network shown in Figure 7(a). Incidentally, this network has $\mathbf{D}_4 \times \mathbf{S}_2$ symmetry. The general system of equations based on this network

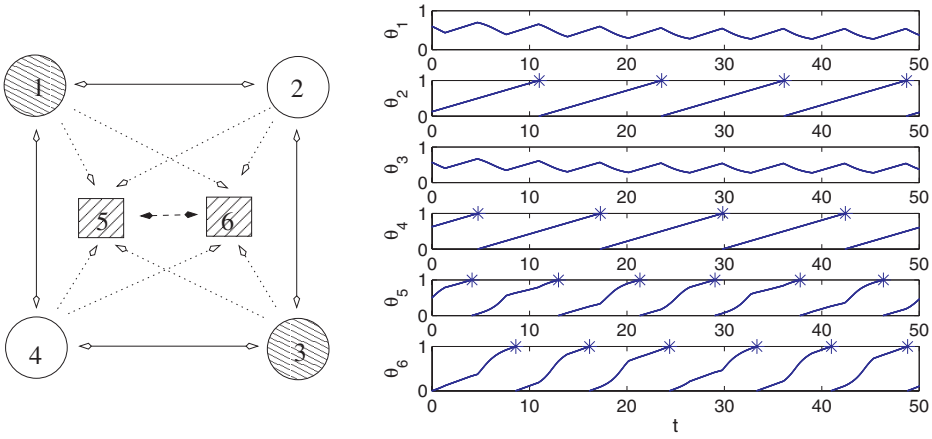

(a) (b)

Fig. 7. (a) Network architecture with $\mathbf{D}_4 \times S_2$ symmetry. There are three coevolving cell pairs: $\{1, 3\}$, $\{2, 4\}$, and $\{5, 6\}$. (b) Simulated trajectories for (4.1) with $\alpha_{5,6} = \alpha_{6,5} = -\frac{0.13}{2\pi}$, $\alpha_{i,j} = -\frac{1.3}{2\pi}$ for connections between the oscillators in the outer ring, and $\alpha_{i,j} = \frac{1.3}{2\pi}$ for connections from the outer to the inner ring (these are chosen to be unidirectional). The remaining $\alpha_{i,j}$ are set to 0. Cell pair $\{1, 3\}$ exhibits subthreshold oscillations; cell pair $\{2, 4\}$ spikes four times on this interval; and cell pair $\{5, 6\}$ spikes six times.

architecture has the form

$$\begin{aligned}
\theta_1' &= f(\theta_1, \overline{\theta_4, \theta_2}),\\
\theta_2' &= f(\theta_2, \overline{\theta_1, \theta_3}),\\
\theta_3' &= f(\theta_3, \overline{\theta_2, \theta_4}),\\
\theta_4' &= f(\theta_4, \overline{\theta_3, \theta_1}),\\
\theta_5' &= g(\theta_5, \theta_6, \overline{\theta_1, \theta_2, \theta_3, \theta_4}),\\
\theta_6' &= g(\theta_6, \theta_5, \overline{\theta_1, \theta_2, \theta_3, \theta_4}),
\end{aligned} \tag{4.4}$$

where $f(a, b, c) = f(a, c, b)$ and g is invariant under any permutation of cells 1–4. It is easy to check that the tori

$$Y_1 = \{\theta \in \mathbf{T}^6\colon\ \theta_1 = \theta_3\}, \qquad Y_2 = \{\theta \in \mathbf{T}^6\colon\ \theta_2 = \theta_4\}, \qquad Y_3 = \{\theta \in \mathbf{T}^6\colon\ \theta_5 = \theta_6\},$$

as well as the 3-torus $Y = Y_1 \cap Y_2 \cap Y_3$ are flow-invariant. It follows that the pairs (1, 3), (2, 4), and (5, 6) each (separately) coevolve. Figure 7(b) illustrates these dynamics, using the form of the coupled system in Example 4.2. In particular, note that there are three different winding numbers in this network, as permitted by Proposition 2.4.

Restricting the system to the torus Y, in which the oscillators are grouped into three synchronous clusters, we can conclude even more about the system. If $\theta_1, \theta_2, \theta_5$ are taken as representatives of the clusters, then (4.4) restricted to Y becomes

$$\begin{aligned}
\theta_1' &= f(\theta_1, \overline{\theta_2, \theta_2}),\\
\theta_2' &= f(\theta_2, \overline{\theta_1, \theta_1}),\\
\theta_5' &= g(\theta_5, \theta_5, \overline{\theta_1, \theta_2, \theta_1, \theta_2}).
\end{aligned} \tag{4.5}$$

The restricted equations (4.5) are the general system that corresponds to the *quotient network* in Figure 8(a). The quotient network can be obtained by projecting all cells in a synchronous cluster to a single cell, and projecting all arrows between these cells in a consistent manner. It will be shown in Section 6 that the resulting graph can be used to obtain the following conclusions, which we obtain here by examining directly the form of the ODEs.

The 2-torus $X = \{(\theta_1, \theta_2, \theta_5) \in \mathbf{T}^3\colon\ \theta_1 = \theta_2\}$ is a codimension-one flow-invariant torus for (4.5). Hence, the cluster phases θ_1 and θ_2 coevolve; that is, any solution of (4.4) lying in Y has the property that either $\theta_1(t) = \theta_2(t)$ or $\theta_1(t) \neq \theta_2(t)$ for all t. This is not the case for solutions that do not lie in Y (when the oscillators do not form synchronous clusters).

Using these observations, and following the arguments of the preceding examples, we can conclude that if the oscillators form synchronous clusters $\theta_1(t) = \theta_3(t)$, $\theta_2(t) = \theta_4(t)$, and $\theta_5(t) = \theta_6(t)$, then the average frequencies of oscillations must be the same, and their winding numbers differ at most by 1. The reader can check that the last conclusion holds even when $\theta_1 = \theta_3$, $\theta_2 = \theta_4$, but $\theta_5(t) \neq \theta_6(t)$ in this system. Figure 8 illustrates the dynamics of these clusters. Compared with the dynamics before forming the three synchronous clusters (Fig. 7), we see that now cells 1, 2, 3, and 4 have the same frequency (here, zero). In general there is no relation between the average frequencies of the cells in the outer ring and the inner cells.

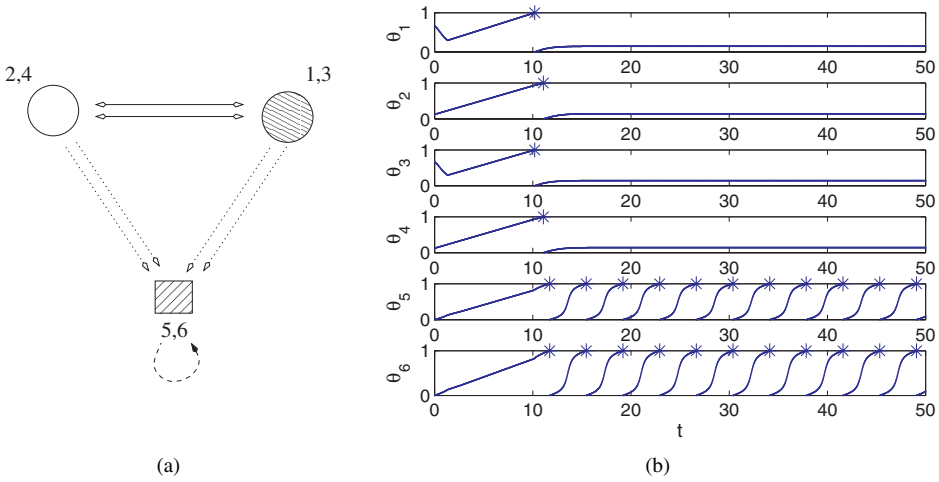

Fig. 8. When coevolving oscillators form synchronous clusters given by the coloring shown here, additional frequency relations must exist. These are obtained by considering the quotient network (a), which results from collapsing all cells in synchronous clusters to a single cell. In this case the two groups of oscillators (1,2,3,4) and (5,6) share the same frequency (that of the first group being zero), while there is no set relation between the frequency of these groups (b).

Next we show that the upper bound discussed in Corollary 3.3 may in fact be achieved.

Example 4.5. As discussed in Section 2, for the network architecture depicted in Figure 1 the cell pairs $(1, 2)$ and $(1, 3)$ coevolve, whereas the cell pair $(2, 3)$ does not. Figure 9 shows the time series for three cells in a particular example of such a network. Note that on the given interval cells 1, 2, and 3 spike one time, zero times, and two times, respectively. Therefore the spike numbers of cells 2 and 3 differ by 2, which is the upper bound given in Corollary 3.3(a).

5. Balanced Relations and Coevolution

While Definition 2.2 is straightforward, it does not provide a direct way of checking when two cells coevolve. In this section we show how network architecture can be used to determine when two oscillators i and j coevolve, that is, to show when $\theta_i = \theta_j$ is flow-invariant. The theory of coupled cell networks developed in [28], [15] leads to two theorems that will allow us to do this in general, as well as to extend the results of Section 2 to synchronous clusters (see Example 4.4). The first theorem (Theorem 5.5) states that polydiagonals (subsets of the torus $\mathbf{T}^N$ defined by the equality of certain coordinates) are flow-invariant for all cell systems with a given network architecture if and only if the equivalence relation that defines the polydiagonal satisfies a network combinatorial condition of a "balanced coloring." The second theorem (Theorem 6.1) states that a restriction of a coupled cell system to a flow-invariant polydiagonal representing the synchronous clusters defines a vector field that itself corresponds to a coupled cell

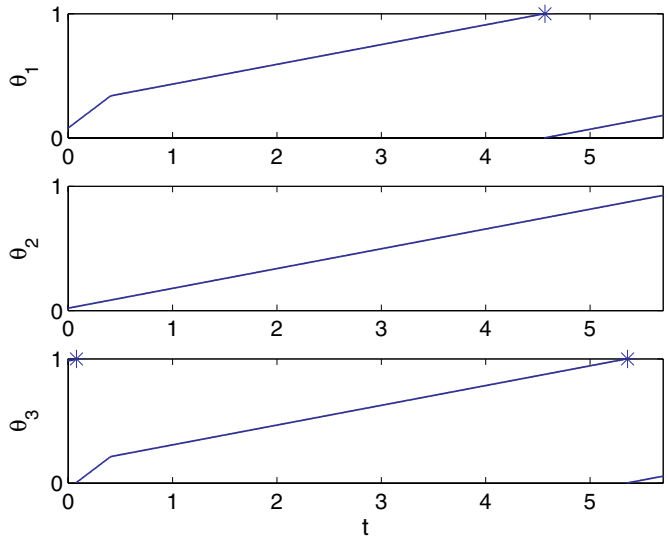

Fig. 9. Trajectories for the three oscillators of the network of Figure 1. The ODEs have the form of (4.1), but with $z(\theta_i)$ itself having a smooth, pulsed form identical to that given in (4.2) (with width parameter for $z(\theta_i)$ chosen to be $c = 0.5$). As in other examples, $g(\cdot)$ is also of the form of (4.2), $\omega = \frac{1}{2\pi}$, $c = \frac{0.5}{2\pi}$, and α_{ij} equal to either $\frac{3}{2\pi}$ or 0 as per the architecture of Figure 1.

system, the *quotient network*. Moreover, the coupled cell vector fields associated with the quotient network exactly determine the possible restricted vector fields.

We use these two theorems as follows. The first theorem allows us to determine when the polydiagonal $\{\theta\colon\ \theta_i = \theta_j\}$ is flow-invariant, as described in Corollary 5.6, the main result of this section. The second theorem allows us to determine when *clusters of synchronous oscillators* coevolve by checking whether certain equivalence relations on the quotient network are balanced. The restrictions on rotation and oscillation numbers described in Section 2 for pairs of coevolving oscillators also hold for coevolving clusters of oscillators, allowing us to complete the present characterization of restrictions on network dynamics.

Although it is well known that symmetries of the network result in *synchrony*, it is less well known that network architecture properties other than symmetry can do the same. As we have shown in Example 4.3, the polydiagonal $\{\theta \in \mathbf{T}^3\colon\ \theta_1 = \theta_2\}$ is flow-invariant for all equations of the form (4.3) associated with the three-cell asymmetric network. The results, developed in [28], [15] and explained below, can therefore be viewed as an extension of the theory of symmetric networks.

5.1. Coupled Cell Networks and Groupoids

We begin our discussion by recalling part of the theory developed in [15]. In this paper a coupled cell network is a coded directed graph where each node symbol represents a

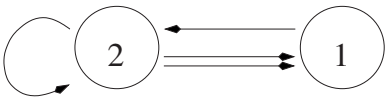

Fig. 10. Two cell network with self-coupling and multiple arrows.

system of differential equations and each arrow symbol represents a type of coupling. Arrows emanate from a *tail* cell, and end at a *head* cell. For example, a network that contains two types of node symbol and three types of arrow symbol is shown in Figure 7.

The *input set* $I(c)$ of a node or cell c is the set of all cells that are connected to c by some arrow pointing to cell c. To be more precise, every cell $b \in I(c)$ is identified with one arrow from b to c.

Note that we allow the possibility of self-coupling (that is, $c \in I(c)$) and multiple couplings from cell d to cell c (that is, d may appear in $I(c)$ multiple times, if there is more than one arrow from cell d to cell c). See Figure 10, where $I(2) = \{2, 1\}$, and $I(1) = \{2, 2\}$. These generalities may at first seem strange, but they are natural when considering quotient networks. We do require one consistency condition: two arrows of the same type must have head cells of the same type and tail cells of the same type.

Our goal is to associate with each coupled cell network a set of admissible systems of differential equations. To do this, we need to make precise the idea that two cells have isomorphic input sets. Two cells c and d are *input equivalent* if there is an arrow type preserving bijection β: $I(c) \to I(d)$, that is, for each cell $b \in I(c)$ the type of arrow between b and c is the same as the arrow type between $\beta(b)$ and d. It follows from the consistency condition that if there is an input isomorphism between the input sets of two cells c and d, then c and d must be of the same type.

We denote the set of input isomorphisms from cell c to cell d by $B(c, d)$. Note that $B(c, c)$ is a group, called the *vertex group*.

Example 5.1. To appreciate the importance of input sets in determining the existence of synchrony subsets, consider again the network in Figure 6. While this system has no symmetries, there is an isomorphism taking all cells that provide inputs to cell 1 to cells that provide inputs to cell 2 (see Figure 11), in the sense that cells of equal types can be mapped to each other. Below we discuss the consequences of this isomorphism for the network dynamics.

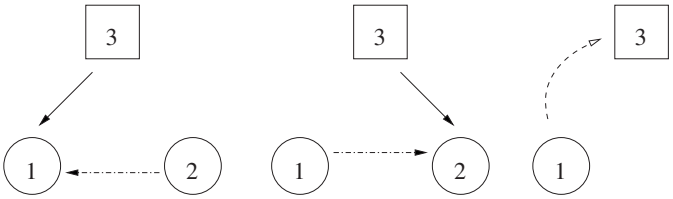

Fig. 11. The input sets for the three cells in the network shown in Figure 6.

5.2. Coupled Cell Phase Equations

In this section we discuss how the general equations modelling coupled cell systems are fully determined by the input sets of the cells in the network, and all isomorphisms between these input sets. This follows the treatment in [28].

Given an ordered subset $I = \{i_1, \ldots, i_s\}$ of cells, where the cell indices can repeat, let

$$\theta_I = (\theta_{i_1}, \ldots, \theta_{i_s}).$$

The *admissible* differential equations associated with a coupled cell network have the form

$$\theta_i' = f_i(\theta_i, \theta_{I(i)}), \tag{5.1}$$

where $I(i)$ is the input set of cell i satisfying the following "groupoid" restriction. Let $\beta\colon I(i) \to I(j)$ be an input isomorphism. Then

$$f_i(\theta_i, \theta_{I(i)}) = f_j(\theta_i, \theta_{\beta^{-1}(I(j))}). \tag{5.2}$$

Note that the equation for cell i is invariant under the vertex group $B(i, i)$; that is,

$$f_i(\theta_i, \theta_{I(i)}) = f_i(\theta_i, \theta_{\beta^{-1}(I(i))}).$$

Example 5.2. Consider the two-cell network in Figure 10, where $I(1) = \{2, 2\}$ and $I(2) = \{1, 2\}$, so that the corresponding ODEs have the form

$$\begin{aligned} \theta_1' &= f_1(\theta_1, \theta_2, \theta_2), \\ \theta_2' &= f_2(\theta_2, \theta_1, \theta_2). \end{aligned} \tag{5.3}$$

By considering the input isomorphisms, we further refine the form of the ODEs. These bijections include (among others): $\beta_1 \in B(2, 2)$, for which $\beta_1(1) = 2$ and $\beta_1(2) = 1$, and $\beta_2 \in B(1, 2)$, for which $\beta_2(2) = 1$ and $\beta_2(2) = 2$. The admissibility condition (5.2) for β_1 implies $f_2(\theta_2, \theta_1, \theta_2) = f_2(\theta_2, \theta_2, \theta_1)$, whereas the admissibility condition for β_2 implies $f_2(\theta_2, \theta_1, \theta_2) = f_1(\theta_2, \theta_1, \theta_2)$. Together this shows that the general form of admissible vector fields for the network in Figure 10 is

$$\begin{aligned} \theta_1' &= f(\theta_1, \overline{\theta_2, \theta_2}), \\ \theta_2' &= f(\theta_2, \overline{\theta_1, \theta_2}), \end{aligned} \tag{5.4}$$

where the overbar indicates that $f\colon \mathbf{T}^3 \to \mathbf{R}$ satisfies $f(a, b, c) = f(a, c, b)$.

5.3. Balanced Colorings and Robust Polysynchrony

Next, we use the ideas developed above to prove Corollary 5.6, which allows us to test when two oscillators coevolve. A *coloring* is obtained by assigning a color to each cell in the network. The notion of a *balanced coloring* is of fundamental importance in our discussion.

Definition 5.3. A coloring is *balanced* if for every pair of cells c and d with the same color there is a color-preserving input isomorphism β: $I(c) \to I(d)$. That is, b and $\beta(b)$ have the same color for every $b \in I(c)$.

For example, the coloring of the network in Figure 8(a) is easily seen to be balanced. Note that if two cells in a balanced coloring have the same color, then these cells must be input equivalent.

A coloring can be viewed as an equivalence relation. We write $i \bowtie j$ if the two cells i and j share the same color. There is a 1:1 correspondence between colorings and polydiagonals, where the *polydiagonal* associated with a coloring $\bowtie$ is the subset of $\mathbf{T}^N$ defined by

$$\Delta_{\bowtie} = \{\theta \in \mathbf{T}^N\colon\ \theta_c = \theta_d \text{ whenever } c \text{ and } d \text{ have the same color}\}.$$

The polydiagonal $\Delta_{\bowtie}$ is a torus in the phase space $\mathbf{T}^N$ of the entire network with dimension equal to the number of equivalence classes defined by the coloring $\bowtie$. The lift $\Delta^L_{\bowtie}$ of $\Delta_{\bowtie}$ to $\mathbf{R}^N$ is therefore a linear subspace.

Definition 5.4. Let $\bowtie$ be a coloring on a coupled cell network. Then $\bowtie$ is *robustly polysynchronous* if $\Delta_{\bowtie}$ is flow-invariant under every admissible vector field.

Equivalently, if $\bowtie$ is robustly polysynchronous, then trajectories $\theta(t)$ for any admissible vector field have the following property: when initial conditions $\theta(0) \in \Delta_{\bowtie}$, then $\theta(t) \in \Delta_{\bowtie}$ for all $t \in \mathbf{R}$.

The following theorem, proved for ODEs in Euclidean spaces in [15] and here adapted to phase oscillator networks, shows the importance of balanced colorings in determining invariant subspaces in the network of the system.

Theorem 5.5. *Let $\bowtie$ be a coloring on a network of phase oscillators. Then $\bowtie$ is robustly polysynchronous if and only if $\bowtie$ is balanced.*

Proof. Theorem 4.3 in [15] states that this theorem is valid for systems of ODEs with Euclidean phase spaces. As noted previously, any phase oscillator system $\theta' = F(\theta)$ can be lifted to an ODE system $x' = F^L(x)$. The lifted system is an admissible vector field for the same network but with phase spaces $\mathbf{R}$ rather than $\mathbf{T}^1$.

First, observe that the torus $\Delta_{\bowtie} \subset \mathbf{T}^N$ is flow-invariant for F if and only if the subspace $\Delta^L_{\bowtie} \subset \mathbf{R}^N$ is flow-invariant for the lift F^L. Second, note that the phase network and the ODE network correspond to identical graphs and that being balanced is a combinatorial property only of the graph. It follows that if the phase oscillator network is balanced, then the ODE network is balanced, the subspace $\Delta^L_{\bowtie}$ is robustly polysynchronous, and the torus $\Delta_{\bowtie}$ is robustly polysynchronous.

To prove the converse we must show that if the torus $\Delta_{\bowtie}$ is flow-invariant for all phase oscillator systems, then the subspace $\Delta^L_{\bowtie}$ is flow-invariant for all admissible vector fields—not just lifted vector fields. Then Theorem 4.3 in [15] would imply that $\bowtie$ is balanced. However, a subspace is flow-invariant globally if it is locally flow-invariant, and locally every admissible ODE is the lift of a phase oscillator system (namely, the

local projection of the vector field on $\mathbf{R}^N$ to the torus $\mathbf{T}^N$), so we have the required result. □

It is easy to check that the equalities used to define the invariant subspaces Y in Examples 4.3 and 4.4 define a balanced coloring. This fact is also a consequence of Theorem 5.5, since we have shown that the equivalence relations used to define these subspaces were robustly polysynchronous.

Next we use Theorem 5.5 to provide a simple test to determine when two cells coevolve. Given two different cells i and j, define the coloring $\bowtie_{i,j}$ so that cells i and j have the same color and all other cells have distinct colors.

Corollary 5.6. *Two cells i and j coevolve if the coloring $\bowtie_{i,j}$ is balanced.*

Proof. Theorem 5.5 implies that $\Delta_{\bowtie_{i,j}} = \{\theta \in \mathbf{T}^N\colon\ \theta_i = \theta_j\}$ is flow-invariant. □

For a given system of phase equations, two cells may coevolve even when $\bowtie_{i,j}$ is not balanced. However, Theorem 5.5 shows that such examples are not robust and are hence atypical. The following proposition provides a direct way of checking whether a coloring $\bowtie_{i,j}$ is balanced.

Proposition 5.7. *Let i and j be cells. Then the coloring $\bowtie_{i,j}$ is balanced if and only if every other cell in the network connects to both cells i and j with the same number (which may be zero) of arrows of each type, and the arrows from i to j are the same in number and type as those from j to i.*

6. Quotient Networks

Using Theorem 5.5, the only synchronous clusters that are robust for a given network architecture are defined by a balanced coloring $\bowtie$. In this section we show that restrictions exist on the rotation and oscillation numbers of synchronous clusters in a network. These restrictions are found by analyzing coevolution on an associated quotient network $\mathcal{G}_{\bowtie}$ defined by $\bowtie$, as in [15].

Example 4.4 illustrated how this process works in a sample network. In that example we found the equations that govern the evolution of certain synchronous clusters explicitly by restricting the equations to the invariant torus defined by those synchronous clusters. We also showed that these restricted equations describe the evolution of a "quotient network" which is determined by the given pattern of synchrony.

We now describe the formal procedure for deriving the architecture of the quotient network. Let $\bowtie$ be a balanced equivalence relation on a coupled cell network $\mathcal{G}$. The cells of the *quotient network* $\mathcal{G}_{\bowtie}$ are the colors (or, more formally, the $\bowtie$ equivalence classes) in the balanced coloring. Observe that in Example 4.4 the cells in the quotient network Figure 8(a) are in 1:1 correspondence with the colors in Figure 7(a).

The arrows in the quotient network are found as follows. Choose a cell $[c]$ in the quotient network that corresponds to a color, and choose a cell c in the original network

that has that color. The input arrows of $[c]$ are the input arrows of c. The tail of a quotient arrow is just the color of the tail cell of that arrow in the original network. The assumption that $\bowtie$ is balanced is sufficient to guarantee that the choice of quotient arrows is independent of which cell c of a given color is used.

Observe, for example, that there are five arrows in the quotient network in Figure 8(a) whose arrow head is the square cell labelled 5, 6. These arrows are just the five arrows whose heads are cell 6 in Figure 7(a). Moreover, one of the arrows entering cell 6 comes from cell 5, and the other four arrows divide into pairs, with each pair consisting of arrows whose tails are cells of the same color.

Finally, the phase space of the quotient network is just the torus $\Delta_{\bowtie}$. The following theorem is proved in [15] for ODEs in Euclidean spaces.

Theorem 6.1 ([15]). *Let $\bowtie$ be a balanced coloring on a coupled cell network $\mathcal{G}$.*

(a) *The restriction of a $\mathcal{G}$-admissible vector field to $\Delta_{\bowtie}$ is $\mathcal{G}_{\bowtie}$-admissible.*
(b) *Every $\mathcal{G}_{\bowtie}$-admissible vector field on the quotient lifts to a $\mathcal{G}$-admissible vector field on the original network.*

Lifted vector fields induced in Euclidean space by $\mathcal{G}$-admissible phase equations are admissible if and only if the phase equations are admissible. Theorem 6.1 then follows immediately from [15, Theorem 5.2].

Theorem 6.1 implies that dynamical properties of synchronous trajectories on the original network can be correctly inferred from the quotient network. In particular, part (a) shows that coevolution in the quotient network imposes restrictions on synchronous dynamics in the original network. Furthermore, part (b) implies that the only restrictions on synchronous dynamics in the original network that hold for all admissible vectorfields may be inferred from the quotient network itself, because admissible vector fields on the quotient always lift.

As an example of a balanced coloring, consider the three-cell bidirectional ring in Figure 12, number the cells 1, 2, and 3, and color cells 2 and 3 red and cell 1 blue. Note that all arrows in this network are of the same type. The quotient network consists of two cells (red and blue). To define the arrows in the quotient network, choose a representative from each color, and simply keep all the input arrows. The blue cell therefore receives two arrows from the red cell, whereas the red cell receives one arrow from a red cell and one arrow from a blue cell. That is, the quotient network is just the two-cell network with self-coupling and multiple arrows shown in Figure 10.

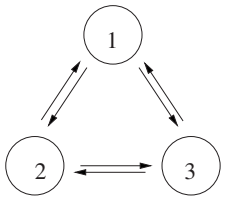

Fig. 12. A bidirectional three-cell ring.

The following is a generalization of Definitions 2.2 and 2.7 to clusters of synchronous cells

Definition 6.2. For a balanced coloring, a *synchronous cluster* consists of all cells of a given color. Two synchronous clusters *coevolve* if the corresponding cells in the quotient network coevolve. Two clusters i and j are in the same *collection* if there exists a *chain* of distinct synchronous clusters $i = k_0, \ldots, k_{m+1} = j$ such that all pairs $(k_0, k_1), \ldots, (k_m, k_{m+1})$ coevolve.

Since all oscillators in a synchronous cluster are synchronous, the winding and spike numbers of a member of a cluster can be used to define these numbers for the entire cluster. The desired restriction on these numbers now follows immediately from applying Propositions 2.3, 2.4, and 3.2 and Corollary 2.8 to the quotient network:

Proposition 6.3. *Fix a balanced coloring in a phase oscillator network. Then,*

(a) *Coevolving synchronous clusters in the same collection have equal winding numbers for a periodic solution.*
(b) *If the average frequency for one synchronous cluster in a collection is defined, then it is defined and is equal for all synchronous clusters in the collection.*
(c) *For a general solution defined on an interval τ, coevolving clusters have winding numbers that differ at most by* 1. *Winding numbers of oscillators in the same collection differ at most by m, the length of the shortest chain relating them.*

It follows, as we saw in Example 4.4, that coevolution in quotient networks can add restrictions on the winding and spike numbers of synchronous solutions that cannot be obtained from coevolution in the original network.

7. Coupling via Buffer Cells and "Synaptic" Variables

In applications it is often the case that phase oscillators interact through auxiliary variables which describe the time course of the coupling, such as synaptic conductances in neural network models. We now show that the results of the previous sections may be extended to this case.

In the case of phase oscillator models of neuronal networks, the effect of a spike in a presynaptic neuron θ_i may be described by introducing a synaptic variable $s_i \in \mathbf{R}^s$ [6]. This variable is introduced because the time course of θ_i after a spike may be influenced by the input from other neurons in the network. On the other hand, the time course of a synaptic conductance is assumed to depend only on the history of the presynaptic neuron. Additionally, delays can be modelled by introducing an auxiliary phase variable θ_i^d satisfying

$$\frac{d}{dt}\theta_i^d = \frac{1}{\tau}(\theta_i^d - \theta_i),$$

and connecting θ_i^d rather than θ_i to other cells in the network. More variables can be

added to better approximate a delayed version of the variable θ_i. We treat any auxiliary coupling variables such as the s_i and θ_i^d as *intermediate* or *buffer* cells in the network.

For simplicity, assume that we begin with a homogeneous network of N phase oscillators with just one type of coupling arrow. Therefore all cells and all arrows in the original network are equivalent. We form a new network by inserting one buffer cell for each "phase" cell in the original network. Each phase cell is connected by one arrow to its companion buffer cell, and each arrow in the original network connecting phase cell c to phase cell d is now replaced by an arrow from the buffer cell companion of c to phase cell d. In the new network, all buffer cells are equivalent and all arrows from phase cells to buffer cells are equivalent. The new network has two types of cell (phase and buffer) and two types of arrow (phase to buffer and buffer to phase). Finally, we assume that buffer cells evolve in a state space $\mathbf{M}$, which equals either $\mathbf{R}^s$ or $\mathbf{T}^s$ (or a product) with $s \geq 1$. The state space of the new network is $\mathbf{T}^N \times \mathbf{M}^N$.

Two examples of homogeneous networks with associated buffer cells networks are shown in Figures 13 and 14. We ask how the existence of buffer cells (modelling synaptic communication or delays in transmission) changes the way phase cells coevolve, and show through these examples that the answer depends on the original network.

The analog of Theorem 5.5 for the state space $\mathbf{T}^N \times \mathbf{M}^N$ implies that the condition for coevolution of phase oscillator pairs remains unchanged: phase oscillators i and j coevolve if the coloring $\bowtie_{i,j}$ is balanced. In the case of a phase oscillator network with buffer cells, $\bowtie_{i,j}$ denotes the coloring in which only cells θ_i and θ_j share the same color. Moreover, Propositions 2.3, 2.4, 3.2, and 6.3 carry over directly to networks with buffer cells, by considering lifts from $\mathbf{T}^N \times \mathbf{M}^N$ to Euclidean space.

Proposition 5.7 implies that when direct connections between oscillators are replaced by indirect connections via intermediate cells, balanced relations may be destroyed, as the following example illustrates.

Example 7.1. Consider the network in Figure 13(b) consisting of two identical phase oscillators θ_1 and θ_2, each of which is identically connected to the other via buffer cells s_1 and s_2:

$$\theta_1' = f(\theta_1, s_2), \quad s_1' = g(\theta_1),$$
$$\theta_2' = f(\theta_2, s_1), \quad s_2' = g(\theta_2).$$

Proposition 5.7 implies that the coloring $\bowtie_{1,2}$ is not balanced because $I(1) = s_2$ and $I(2) = s_1$, so the phase oscillators do not coevolve in general. If the oscillators con-

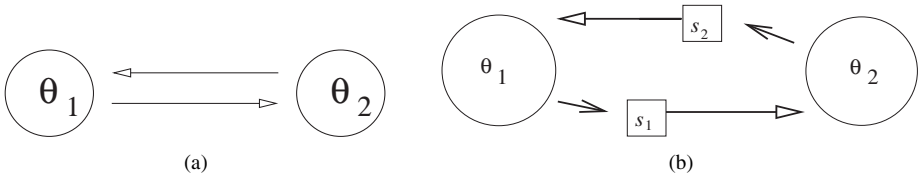

Fig. 13. A network consisting of two identical phase oscillators connected directly (a) and through buffer cells (b).

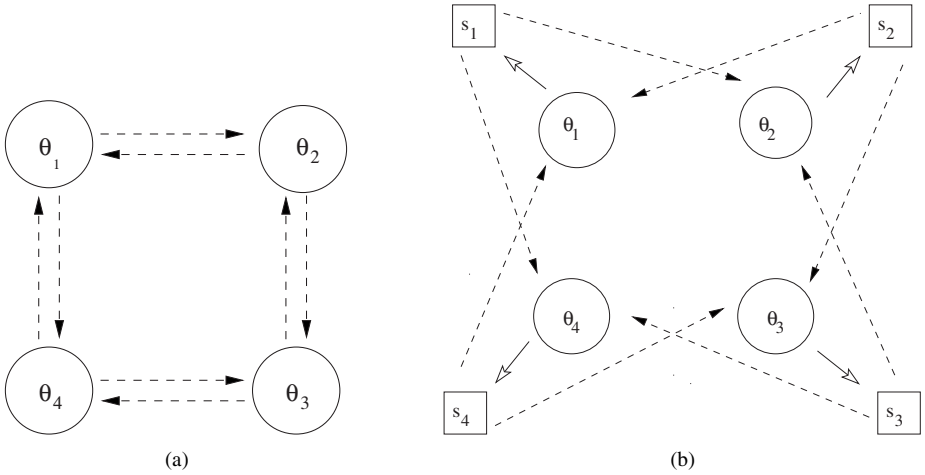

Fig. 14. A $\mathbf{D}_4$ symmetric network a of four identical phase oscillators connected directly (a) and through buffer cells (b).

nected directly without intermediate cells (as in Fig.13(a)), the coloring $\bowtie_{1,2}$ *would* be balanced.

Thus, a balanced coloring can be destroyed by the addition of temporal dynamics in the coupling. However, this is not always the case:

Example 7.2. Consider the network in Figure 14(b) consisting of four identical phase oscillators with $\mathbf{D}_4$ symmetry and four buffer cells. The colorings $\bowtie_{1,3}$ and $\bowtie_{2,4}$ are both balanced, so the corresponding phase oscillator pairs coevolve. These pairs are also the only pairs that coevolve in the original four-cell bidirectional ring in Figure 14(a).

Therefore, in contrast to the previous example, the same pairs coevolve whether coupling takes place through intermediate cells or not. The difference is that in Example 7.1 the coevolving cells in the directly coupled network provide input to each other (via buffer cells), which is not the case in Example 7.2. This observation can be generalized to obtain the following corollary to Proposition 5.7.

Corollary 7.3. *A coloring $\bowtie_{i,j}$ in a network of directly coupled cells remains balanced after the addition of buffer cells if there are no arrows between i and j.*

Remark 7.4. If an arrow from i to j does exist, $\bowtie_{i,j}$ remains balanced if the indirectly coupled network is modified so that buffer cells s_i and s_j provide additional, identical inputs to cells i and j, respectively.

We illustrate Corollary 7.3 and Remark 7.4 using two subtly different realizations of all-to-all (indirect) coupling among phase oscillators.

Example 7.5. Consider a network with $\mathbf{S}_N$ symmetry, in which all oscillators are coupled to all others (except for themselves) via identical intermediate cells:

$$\theta_i' = f(\theta_i, \overline{s_1, s_2, \ldots, s_{i-1}, s_{i+1}, \ldots, s_N}),$$
$$s_i' = g(\theta_i).$$

Each cell receives identical inputs (indirectly) from auxiliary cells corresponding to all of its neighbors, but not from itself. For this network, no colorings $\bowtie_{i,j}$ are balanced, as may be checked using Proposition 5.7. Thus, for general coupled cell systems of this form, *no* cells coevolve. However, if the cells were directly connected (without intermediate cells), then all cells would coevolve as shown previously in Corollary 4.1.

The situation changes dramatically when one adds self-coupling to obtain

$$\dot{\theta}_i = \hat{f}(\theta_i, \overline{s_1, s_2, \ldots, s_N}),$$
$$\dot{s}_i = g(\theta_i).$$

Each cell now receives identical inputs (indirectly) from all other cells in the network, including itself. Then all two-phase colorings in which θ_i and θ_j are assigned the same color are balanced. Thus, for every coupled cell system of this form, *all* cells coevolve.

We close this section by remarking that formalism above can be applied in a straightforward manner to the case in which buffer cells each receive inputs from multiple phase oscillators, as in the case of pre- and postsynaptic influence on synaptic variables; the same test for balanced colorings then gives conditions for coevolution.

8. Discussion and Applications

In [3], codimension-one invariant tori $\{\theta \in \mathbf{T}^N\colon\ \theta_i = \theta_j\}$ are used to define the boundaries of "canonical invariant regions" within which solutions are constrained for $\mathbf{S}_N$ symmetric networks. Here, we extend this general idea to networks with less or no symmetry, focusing on constraints that network structure imposes on arbitrary solutions. The constraints on winding and spike numbers that we identify here, summarized in Corollary 2.8, also have interesting consequences for spatiotemporally symmetric periodic solutions in networks of phase oscillators. These are explored in [11].

Applications of the present results may be made wherever phase descriptions of coupled oscillators arise, but the networks encountered in mathematical biology and neuroscience in particular (where spiking systems arise) seem especially suitable. We see two ways in which our results might be used.

First, the present results provide a design guarantee. No matter how the details of internal or coupling dynamics of a network may change, as long as they respect a specified network architecture, then certain measures of oscillation frequency among cells must be preserved. In this context, our results may apply to central pattern generators studied in the form of small networks responsible for functions ranging from locomotion [13] to digestion [26], or to interacting neural assemblies (rather than individual neurons) involved in higher functions [32]. A related possibility is that the $(b-1)!$ distinct spike orderings that are invariant for ordered collections of oscillators could play a role

in short-term encoding of different signals by spiking neural networks (cf. [30], [24], [1]). These suggestions beg the general question of how structured networks (e.g., with connection strengths drawn from a relatively small number of choices) might arise in neuroscience. Studies of spike-time-dependent plasticity suggest one possibility: Song et al. [27] show that such plasticity can lead to highly structured (in fact, bimodal) distributions of synaptic strengths among the inputs to a single neuron. Further work [18] demonstrates that similar distributions of synaptic strengths arise naturally in large spiking networks; nevertheless, the resultant role of coevolution, if present, remains to be characterized.

The second broad way in which our results may be used is in ruling out certain network architectures as candidate models for physical processes from data. If a pair of cells are observed not to coevolve, then the possible network architectures are restricted.

Our results assume that individual cells are described by a single one-dimensional phase variable. In certain circumstances, higher dimensional systems can be rigorously reduced to this case, and then our conclusions can be applied to the original system (see Appendix). Moreover, even in the presence of small noise in the network of phase oscillators, the "ghosts" of the invariant polydiagonals can be expected to persist, and force *approximate* relations between frequencies averaged over a finite times. On the other hand, the absence of strongly attracting limit cycles (or the presence of relatively strong coupling) can enable higher-dimensional oscillator networks that invalidate the assumptions discussed here.

Acknowledgments

The work of MG and KJ was supported in part by NSF Grant DMS-0244529, and EB was supported by a NSF Mathematical Sciences Postdoctoral Research Fellowship.

A. The Origin of Phase Oscillator Models

Networks of phase oscillators described by (1.1) arise in two ways when modelling physical systems. When one considers networks of Josephson junctions (with negligible capacitance terms), for instance, the actual physical quantity that is modelled is a priori assumed to be one-dimensional and periodic in space. In other cases, mathematical models are simply posited in forms equivalent to phase equations, such as the excitatory LIF equations to be discussed in greater detail below. In such examples, the systems variables are phases, and the architecture of the network of phase oscillators is part of the formulation of the problem.

In other examples, phase oscillator models are obtained by a reduction of more complicated equations involving networks of systems, each of which originally evolves in a space larger than $\mathbf{S}^1$. That is, the reduction to phase equations starts with a network of cells $x = (x_1, x_2, \ldots, x_N)$, where each $x_i \in \mathbf{R}^M$, and

$$x_i' = g_i(x) \quad \text{(or equivalently } x' = G(x)\text{)}. \tag{A.1}$$

If the individual cells composing the network oscillate periodically when taken out of the network, each oscillator traces out a topological circle in its phase space. The direct

product of these circles defines an invariant torus for the network of uncoupled oscillators. Similar arguments may be made for "excitable" systems that do not oscillate independently, but possess attracting invariant curves [17]. In either case, under appropriate conditions, the torus persists for the coupled network. Approximate equations governing the evolution on the perturbed torus take the form of phase equations. In this section we review the derivation of certain phase oscillator models that are obtained in this way, and that were used as examples in the previous sections.

An important question is whether the reduced equations thus obtained retain the structure of the original equations (A.1). For instance, will the reduced equations exhibit the symmetries of the original equations? If oscillator i and j are coupled in the original equations, will they be coupled in the reduced equations? Will input isomorphisms persist? We show that in most examples found in practice, the answer to both questions is yes.

A.1. Reduction to Phase Coordinates

In this section we discuss the typical situations in which equation (A.1) can be reduced to an equation of type (1.1). We also discuss the structure that the reduced equation inherits from the full equation.

Phase reduction is most commonly performed in networks of weakly coupled systems [19], [20], [17], [21], [8], [23], each of which is assumed to oscillate with a unique limit cycle when uncoupled from the rest of the network. Such networks are commonly modeled by equations of the form

$$x_i' = f_i(x_i) + \varepsilon G_i(x), \quad i = 1, \dots N, \tag{A.2}$$

where $x = (x_1, x_2, \dots, x_N)$ and $x_i \in \mathbf{R}^M$. The small parameter ε determines the strength of coupling among the oscillators. Standard results from the theory of normally hyperbolic invariant manifolds [20], [9] show that the torus $\mathcal{T}_0$ formed by the product of the limit cycles of the individual oscillators when $\varepsilon = 0$ is perturbed to a unique, nearby torus $\mathcal{T}_\varepsilon$ for small ε. In this situation, reduction to a system of phase equations is possible, and the equations are computable to any order in ε. Importantly, the torus $\mathcal{T}_0$ also persists when the coupling between the oscillators is weak compared to the contraction to the limit cycle in an individual oscillator; thus, the reduction may continue to be valid for nonweak coupling in the phase equations.

Suppose that some of the oscillators in the network are identical (i.e., that $g_i = g_j$ for certain combinations of i and j), so that the network of oscillators possesses a particular permutation symmetry. By this we mean that there is a group Γ that acts on $\mathbf{R}^{MN}$, by permuting the oscillators $x = (x_1, \dots, x_N)$, and has the property that $\gamma G(x) = G(\gamma x)$ for all $\gamma \in \Gamma$. Under this assumption, if $x(t)$ is a solution of (A.1), then so is $\gamma x(t)$, and the torus $\mathcal{T}_0$ is invariant under Γ.

Moreover, if $\mathcal{T}_\varepsilon$ is an invariant torus for (A.1), then so is $\gamma\mathcal{T}_\varepsilon$. Since $\mathcal{T}_\varepsilon$ is the unique invariant torus in a neighborhood of $\mathcal{T}_0$ for the perturbed system, and since $\gamma\mathcal{T}_0 = \mathcal{T}_0$ implies that $\gamma\mathcal{T}_\varepsilon$ is also in the neighborhood of $\mathcal{T}_0$, it follows that $\gamma\mathcal{T}_\varepsilon = \mathcal{T}_\varepsilon$ for every $\gamma \in \Gamma$. Therefore, the restriction of (A.2) to $\mathcal{T}_\varepsilon$ is Γ-equivariant.

In practice, the restriction of (A.2) to $\mathcal{T}_\varepsilon$ is rarely computed directly. Instead, one finds approximate equations in the coordinates on $\mathcal{T}_0$. It is therefore necessary to ask

whether these approximate equations are Γ-equivariant. Here we answer more general questions: Is it true that cell i provides an input to cell j in the reduced equations (1.1) (assumed written in the coordinates on $\mathcal{T}_0$) if and only if the same is true in the original system (A.2)? Do cell i and cell j provide the same input to cell k in (1.1) if and only if they provide the same input to k in (A.2)? Theorem 4.7 and the subsequent discussion in [17] shows that the answer is yes to both of these questions, subject to the caveat below. It follows that the reduced equations of the network (1.1) will have the same groupoid structure as the original equations (A.2).

We note a subtlety with our answers in the previous paragraph: they are only valid to lowest order. In particular, the equations describing the phase θ_i of oscillator i on the invariant torus $\mathcal{T}_\varepsilon$ of A.2 may actually depend on the phase θ_j of oscillator j even if the original equation A.2 for x_i does not depend on x_j [17]. However, this dependence will be of order $o(\varepsilon)$, and will therefore not appear in standard forms of the reduced equations, which typically capture only terms up to $\mathcal{O}(\varepsilon)$.

The results we present can therefore be expected to be valid at least on timescales of $\mathcal{O}(1/\varepsilon)$. If the invariant manifolds $\Delta_{k,j} = \{\theta\colon\ \theta_k = \theta_j\}$, which force relations between winding numbers, persist under the addition of $o(\varepsilon)$ terms, then these results are valid for all time for the phases in the unreduced model. The manifolds $\Delta_{k,j}$ can be expected to be only *weakly* normally hyperbolic when the flow of (A.2) is restricted to $\mathcal{T}_\varepsilon$. The persistence of such manifolds is a delicate issue that we do not address here ([5], see also [2]). Finally, we note that the order of additional coupling terms (involving cells outside of the original input sets) scales with the distance of the torus $\mathcal{T}_\varepsilon$ from $\mathcal{T}_0$. Therefore, for a fixed value of ε, in cases in which there is relatively strong contraction to $\mathcal{T}_0$, these additional coupling terms may be expected to be smaller, and hence the results we present valid on longer timescales.

A.2. Phase Response Curves

A useful approximate form of the phase-reduced equations may be derived via a coordinate change to asymptotic or "canonical" phase coordinates [16], [31], [17], [21], [4]. The basic idea is to parameterize the torus $\mathcal{T}_0$ so that the uncoupled (i.e. unperturbed) dynamics are $\dot{\theta}_j = \omega_j$, where ω_j is the natural frequency of the jth oscillator. Expressed in these phase coordinates, equation (A.2) becomes (neglecting terms of order ε^2)

$$\dot{\theta}_i = \omega_i + \varepsilon z_i(\theta_i) \cdot G_i(\theta), \tag{A.3}$$

where $z_i(\theta_i)$ is in general a vector of partial derivatives resulting from the coordinate change. However, in many applications, the perturbations $G_i(\theta)$ affect only a single variable in each cell, so that the final term in (A.3) is simply the product of two scalar valued functions, as we will assume below. In this context $z_i(\theta_i)$ is referred to as the *phase response curve* (PRC), as it describes the susceptibility of the ith cell to external influence as a function of its phase.

In particular, if coupling enters the original equations in the pairwise additive fashion,

$$x_i' = f_i(x_i) + \sum_j \alpha_{ij} G_j(x_j) \qquad i = 1, \ldots N, \tag{A.4}$$

where the coupling coefficients α_{ij} implicitly replace ε as small parameters and the

$G_j(x_j)$ represent the influence of the jth cell, then, again to lowest order in the coupling strength, equation (A.4) becomes

$$\dot{\theta}_i = \omega_i + z(\theta_i) \sum_j \alpha_{ij} g_j(\theta_j) \quad . \tag{A.5}$$

This is the form of the phase equations used in the simulations above. It is especially useful in applications, as the PRCs $z(\theta_i)$ may be chosen to represent, for example, neurons with specific physical properties or near certain bifurcations (see [7], [20], [4] and references therein).

References

[1] P. Ashwin and J. Borresen. Encoding via conjugate symmetries of slow oscillations for globally coupled oscillators. *Phys. Rev. E* **70** (2004) 026203.

[2] P. Ashwin, O. Burilko, Y. Maistrenko, and O. Popovych (in preparation).

[3] P. Ashwin and J. W. Swift. The dynamics of n weakly coupled identical oscillators. *J. Nonlinear Sci.* **2(1)** (1992) 69–108.

[4] E. Brown, J. Moehlis, and P. Holmes. On the phase reduction and response dynamics of neural oscillator populations. *Neural Comp.* **16** (2004) 673–715.

[5] C. Chicone and W. Liu. On the continuation of an invariant torus in a family with rapid oscillations. *SIAM J. Math. Anal.* **31(2)** (1999–2000) 386–415.

[6] P. Dayan and L. Abbott. *Theoretical Neuroscience.* MIT Press, Cambridge, 2001.

[7] G. B. Ermentrout. Type I membranes, phase resetting curves, and synchrony. *Neural Comp.* **8** (1996) 979–1001.

[8] G. B. Ermentrout. *Simulating, Analyzing, and Animating Dynamical Systems: A Guide to XPPAUT for Researchers and Students*. SIAM, Philadelphia, 2002.

[9] N. Fenichel. Persistence and smoothness of invariant manifolds for flows. *Indiana Univ. Math. J.* **21** (1971–1972) 193–226.

[10] W. Gerstner and W. M. Kistler *Spiking Neuron Models.* Cambridge University Press, Cambridge, 2002.

[11] M. Golubitsky, K. Josić, and E. Shea-Brown. *Spatiotemporal symmetries in phase oscillator networks.* In progress.

[12] M. Golubitsky and I. Stewart. *The Symmetry Perspective*, Progress in Mathematics **200**. Birkhäuser Verlag, Basel, 2002.

[13] M. Golubitsky, I. Stewart, P.-L. Buono, and J. J. Collins. A modular network for legged locomotion. *Physica D* **115** (1998) 56–72.

[14] M. Golubitsky, I. N. Stewart, and D. G. Schaeffer. *Singularities and Groups in Bifurcation Theory, vol. 2.* Applied Mathematical Sciences **69**, Springer-Verlag, New York 1988.

[15] M. Golubitsky, I. N. Stewart, and A. Török. Patterns of synchrony in coupled cell networks with multiple arrows. *SIAM J. Appl. Dynam. Sys.* **4**(1) (2005) 78–100.

[16] J. Guckenheimer. Isochrons and phaseless sets. *J. Math. Biol.* **1** (1975) 259–273.

[17] F. Hoppensteadt and E. Izhikevich. *Weakly Connected Neural Networks*. Springer-Verlag, New York, 1997.

[18] E. Izhikevich, J. Gally, and G. Edelman. Spike-timing Dynamics of Neuronal Groups. *Cerebral Cortex*. **14**(8) (2004) 933–944.

[19] C. Koch and I. Segev, eds. *Methods in Neuronal Modeling*. MIT Press, Cambridge, 1998.

[20] N. Kopell and G. B. Ermentrout. Frequency plateaus in a chain of weakly coupled oscillators, I. *SIAM J. Math. Anal.* **15** (1984) 215–237.

[21] Y. Kuramoto. Phase- and center-manifold reductions for large populations of coupled oscillators with application to non-locally coupled systems. *Int. J. Bif. Chaos* **7** (1997) 789–805.

[22] N. Levinson. Small periodic perturbations of an autonomous system with a stable orbit. *Ann. Math.* **52** (1950) 727–738.

[23] T. Lewis and J. Rinzel. Dynamics of spiking neurons connected by both inhibitory and electrical coupling. *J. Comp. Neurosci.* **14** (2003) 283–309.
[24] W. Maass, T. Natschlager, and H. Markram. Real-Time Computing without Stable States: A New Framework for Neural Computation Based on Perturbations. *Neural Comp.* **14** (2002) 2531–2560.
[25] A. Pikovsky, M. Rosenblum, and J. Kurths. *Synchronization: A Universal Concept in Nonlinear Science*. Cambridge University Press, Cambridge, 2003.
[26] A. A. Prinz, D. Bucher, and E. Marder. Similar network activity from disparate circuit parameters. *Nature Neurosci.* **7** (2004) 1345–1352.
[27] S. Song, K. D. Miller, and L. F. Abbott. Competitive Hebbian learning through spike-timing-dependent synaptic plasticity. *Nature Neurosci.* **3** (2000) 919–926.
[28] I. Stewart, M. Golubitsky, and M. Pivato. Symmetry groupoids and patterns of synchrony in coupled cell networks. *SIAM J. Appl. Dynam. Sys.* **2**(4) (2003) 609–646.
[29] S. Strogatz. *Sync: The Emerging Science of Spontaneous Order*. Theia, New York, 2003.
[30] K. Wiesenfeld and P. Hadley. Attractor crowding in oscillator arrays. *Phys. Rev. Lett.* **62** (1989) 1335–1338.
[31] A. T. Winfree. *The Geometry of Biological Time*. Springer, New York, 2001.
[32] Special edition of *Neuron* **7–9** (September 1999).